

High Energy Radiation Detection During Solar Eclipse

Imaad Syed^{ab}, Leonello Castro Cillis^a, Kevin Whiten^a, Ismail Aadan^a, Malcolm Maas^a

Abstract

The April 8th, 2024 Total Solar Eclipse presented a unique opportunity to investigate how the eclipse affects UV and high energy particle radiation. To record relevant data, the team designed a cost-effective open-source payload, consisting of a Geiger Muller (GM) Counter, two UV photodiode sensors, a pressure sensor, and two temperature sensors. These sensors enable the payload to record UV index, high energy particle counts and temperature with respect to the altitude. The payload was launched on a weather balloon before totality to observe the effect of the eclipse on these quantities. It successfully logged data at intervals of approximately 30 seconds but stopped logging shortly before totality. The payload did demonstrate that the UV index generally decreased with altitude leading up to the eclipse and high energy particle counts generally increased with altitude. The payload also successfully generated a temperature profile varying with altitude. The computer program and parts list for this payload have been made available for open-source use.

eclipse | radiation | high altitude balloon | open-source

1. Introduction

High altitude balloons are a method of gathering scientific data in the low Earth atmosphere. Flying payloads on high altitude balloons up to near space allows for many analyses, such as those of temperature, pressure and radiation. Such experiments can be useful in determining what atmospheric conditions look like at a given altitude, location, season, and time of day. High-energy particle detection is an area of interest in high-altitude ballooning, having advanced significantly over the years. In the past, some rather complicated ionization chamber systems were used to obtain radiation profiles [1]. With modern electronics, this process of sensing and data acquisition has become far more streamlined [2]. Several balloon payloads have logged high energy particle counts, showing a general increase as altitude increases, until a critical altitude of ~20,000 m where the counts seem to stabilize [3-4]. This maximum altitude is the Regener-Pfotzer maximum and is documented in literature [5]. Interestingly, data collected from a sounding rocket flight shows a near constant rate for altitudes above around 45 km (this holds true up to the maximum altitude recorded) [6]. This constant rate is also below the count rate at the Regener-Pfotzer Maximum.

Notably, [4] recorded GM Counter counts during the 2017 Total Solar Eclipse. With the 2024 Total Solar Eclipse, it is only natural to collect more radiation data, to build up a store of information and validate results of previous launches during the eclipse. In addition to logging high energy particle counts with a GM Counter, the team found it interesting to log UV radiation data as well.

Radiation, such as ultraviolet, gamma, and cosmic rays, varies significantly with altitude. As these high-energy rays enter the upper atmosphere, the radiation cascades, resulting in much

^aUndergraduate student, University of Maryland, College Park

^bCorrespondence email: isyed1@terpmail.umd.edu

lower-energy forms of light in the lower atmosphere. Common sensors have been implemented on many previous ballooning missions to measure various trends in different kinds of radiation in the low atmosphere [7]. One method is using a GM Counter, which counts high-energy photons and particles. Incident radiation ionizes gas in a high voltage GM tube, resulting in an increasing number of ionizations (avalanche effect). This causes ionization saturation, so any sufficiently high energy radiation produces this charge avalanche. Thus, high energy photons can be counted, at the cost of energy resolution [8].

Other types of scintillators can be used to spectroscopically measure certain high-energy photons by measuring their energy instead of the number of photons. For example, gamma-ray spectroscopy can be done with solid scintillators, often sodium iodide (NaI) or Cesium iodide (CsI). As light passes through the scintillator, its energy gets reduced, often to values in the visible range. The latter process must occur because these lower-energy photons will pass through a photomultiplier tube (PMT) sensitive to lower energies. The PMT uses dynodes, as the incoming number of photons is usually hard to detect, especially for gamma rays [8]. This amplifies the signal when it exits the PMT, providing energy values for the gamma rays.

1.1. University of Maryland Balloon Payload Program

The University of Maryland Balloon Payload Program (UMD-BPP) launches high altitude balloons (HAB) to both collect scientific data beneficial to atmospheric science [4] and address various HAB engineering challenges [9-11]. A highlight of the program is participation in the National Eclipse Ballooning Project (NEBP), where payloads are launched during the solar eclipses of 2023-24. This presented the opportunity to launch the payload during the 2024 Total Solar Eclipse. The program also provides design files to contribute open-source hardware [12]. To give back to the community, it is important to provide software and a list of hardware so that other high altitude balloon enthusiasts (particularly amateurs) can more easily get started with high altitude radiation measurements. The data logging program can be found at [13], with hardware information and a data processing script planned to be released shortly.

2. Payload Design and Methodology

The purpose of this payload was to collect high energy radiation information (GM counts, UV intensity) in a cost-effective manner. Thus, an inexpensive payload was constructed out of common hobby electronics and loaded in a reused foam core casing. Relevant details are described in the following sections.

2.1. Payload Sensors and Electronics

To collect temperature, UV radiation, high energy particle counts, and altitude, an array of sensors are used. A MS5611 pressure sensor records atmospheric pressure, which can then be used to obtain altitude, using the following formula [14]. P_m is the measured pressure, P_s is the reference pressure, which is 1013.25 hPa.

$$H = 0.3048 * \frac{\log_{10}\left(\frac{P_m}{P_s}\right) - 1}{-6.8755856 * 10^{-6}} \quad (1)$$

This sensor also doubles as a temperature measurement unit. A 135-104LAF-J01 thermistor served as a secondary temperature measurement unit, capable of operating at lower temperatures than the MS5611 in case the altitude reached was high enough to exceed its lower

operating temperature bound. While the MS5611 would fail at altitudes greater than 100,000 ft, the thermistor can still operate reliably (thermistor reliable down to a lower bound of -60 C [15]).

Two GUVA-S12SD UV sensors are used to record UV index through feeding an analog signal back to an Arduino Uno microcontroller. The conversion from the ADC bit value to UV index is given below, being adapted from [16]. The k-term is the 10-bit value read from the Arduino's ADC.

$$I_{UV} = 50 * \frac{k_{ADC}}{1024} \quad (2)$$

Finally, for recording high energy particle counts, a LND, Inc. LND-712 GM tube with a NASA/RockOn provided processing circuit board was used. A digital pulse was produced by the GM counter and fed into the Arduino Uno for data capture.

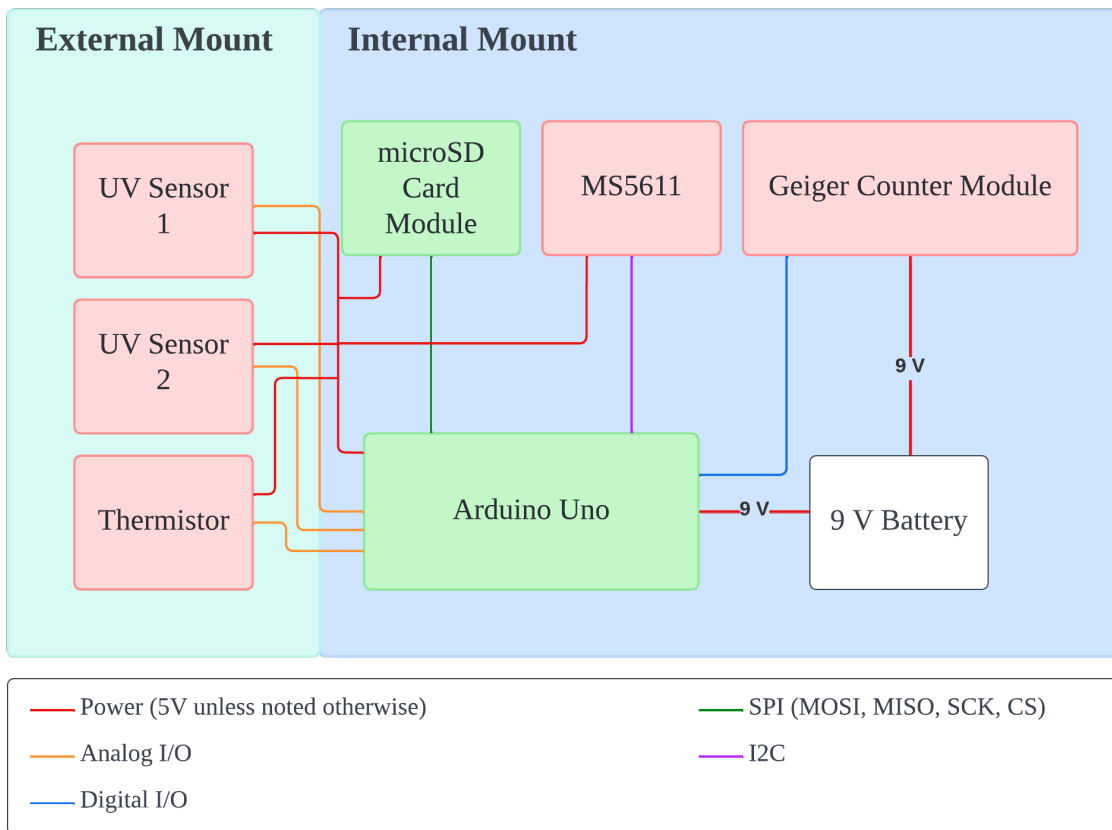


Fig. 1. High level electronics diagram.

The payload's microcontroller is an Arduino Uno, chosen due to its ease of use and low cost. A microSD card module was added for recording data during the flight. The payload used a lithium 9 V battery, to keep weight low. An overall diagram is shown in Fig. 1.

2.2. Payload Software

The data logging program was written for an Arduino Uno microcontroller. The program is summarized in Fig. 2. Data is recorded every 30 seconds, with the final altitude, accumulated

high energy particle count, UV indices, temperature, and altitude logged each time 30 seconds have passed. The delay time in milliseconds is also recorded to normalize the counts. The method of logging high-energy particle counts is like the one described in [4] but uses 30-second logging intervals to get better altitude resolution.

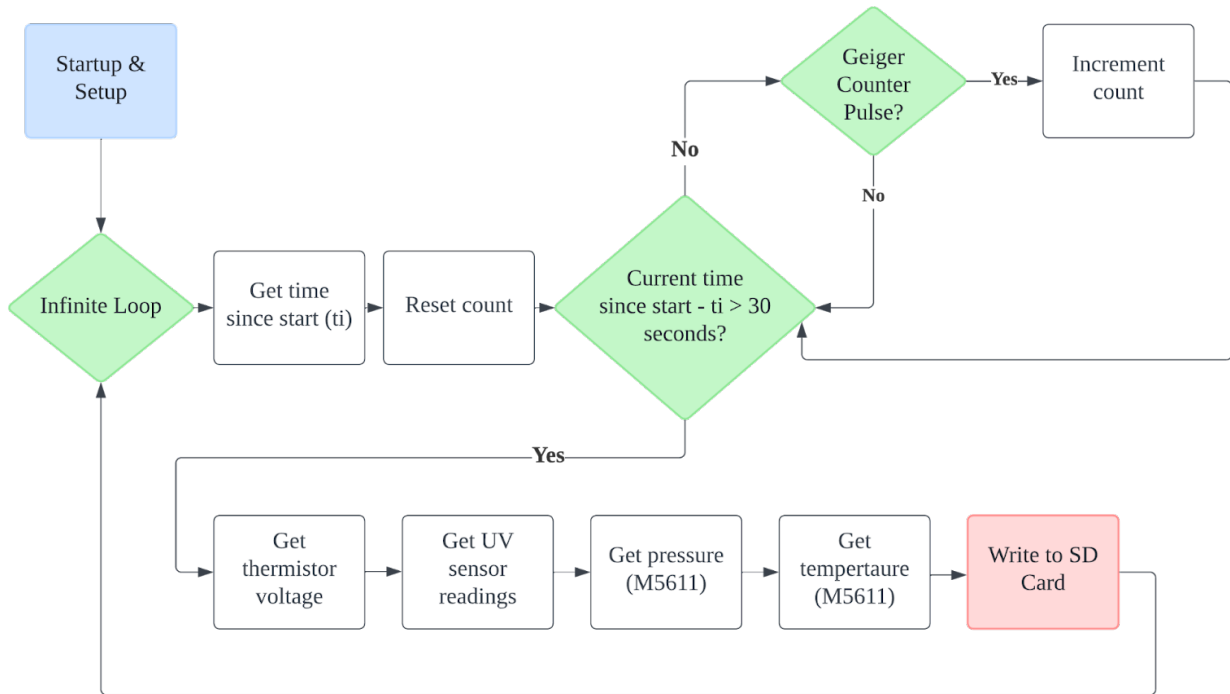


Fig. 2. Software flow diagram.

2.3. Payload Structure

To reduce the weight of the payload, its structure was made using lightweight materials. A structure was provided, being salvaged from a previous payload. The outer walls of the payload were made using 0.5 cm thick foam board put together to make a box. The inside of the payload was insulated using an insulating foam material with a thickness of 1.27 cm to protect the inside components from damage due to falling or shaking. The inside of the payload is accessed via a panel on the side of the payload which is sealed with tape during launch. A hole through the top and bottom faces of the payload allows low-friction tubing to be passed through the center of the payload, which is secured by a pair of washers and pins. This setup allows the payload to be attached to the weather balloon by passing the flight line through the tubing, with the flight line being tied on to a chain of balloon payloads. Three of the sensors – two GUVVA-S12SD UV sensors and a single 135-104LAF-J01 thermistor – were placed on the outside edge of the payload to record the relevant data. Visuals of the payload are provided in Fig. 3.

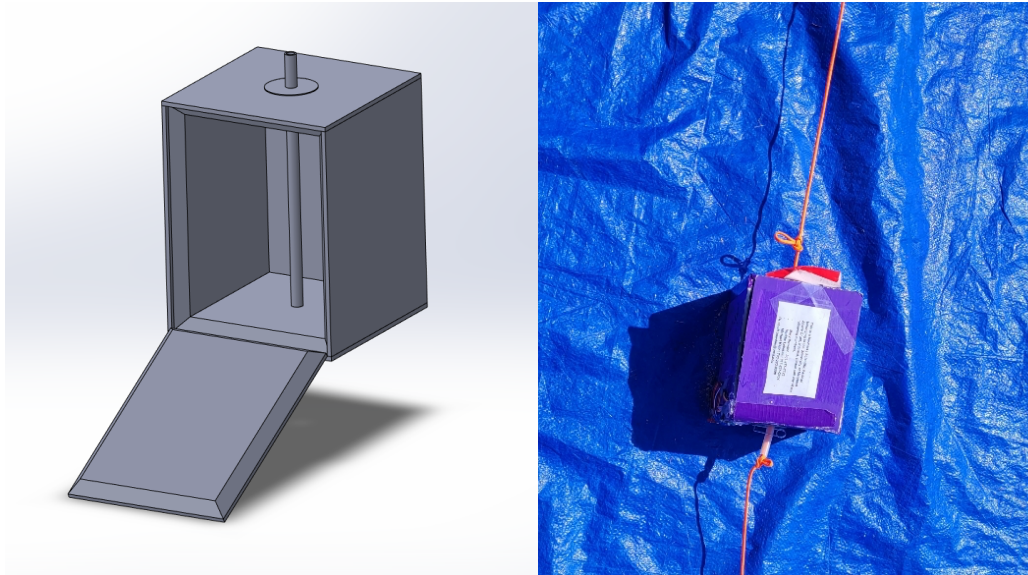


Fig. 3. 3D Model of Payload and photo of actual payload.

2.4. Launch Details



Fig. 4. Photo of high-altitude balloon with all payloads.

The payload was launched on one of two balloons from Portland East Elementary School in Portland, Indiana on April 8th, 2024, at around 2:10 PM (~1 hour before totality). The balloon in question was 1600 g, consisting of 9 total payloads. The presented payload's mass was 340 g, with the mass of all payloads being approximately 4.66 kg in total. As a part of the launch procedure, a plastic tent structure was built, and the balloon was inflated inside of it to account for the relatively windy conditions. This prevented the balloon from flying away too early. After

completing inflation, the payloads were tied on, and the payload presented in this paper was powered up. After being tied onto the flight line, the balloon was slowly allowed to ascend on a tether, before finally being released. A launch photo is found in Fig. 4.

The payload battery died ~1.25 hours after being turned on. The balloon flew up to a maximum height of ~15 km (see Fig. 5 for a complete altitude profile) before descent. The payloads of this balloon ended up landing in trees and were recovered two days later. After retrieval, the payload's structure was seriously weakened by water damage, but the microSD card was successfully recovered.

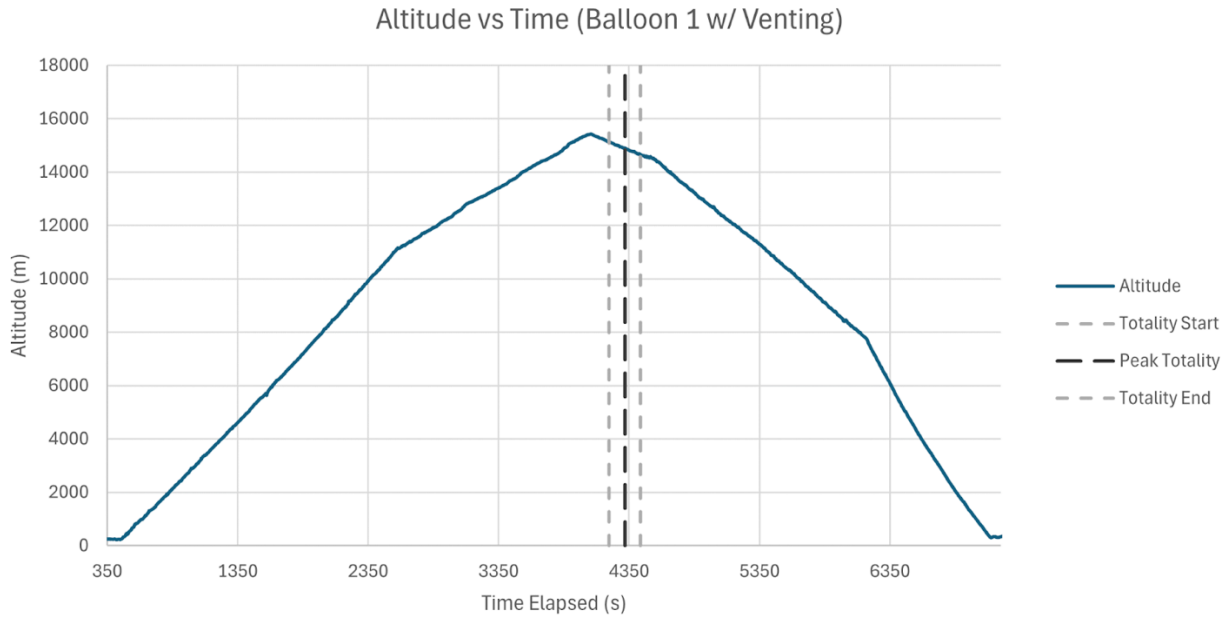


Fig. 5. Balloon altitude profile provided by Akemi Takeuchi of UMD-BPP.

3. Data and Analysis

After the payloads were recovered and brought back to the University of Maryland, the microSD card had logged ~1.26 hours of data into a CSV file. The payload's final recorded altitude before shutdown was ~14249 meters. Raw data included raw ADC readings for the UV sensors and thermistor, temperature and pressure from the MS5611, high energy counts accumulated over 30 second intervals and elapsed time between measurements. The UV ADC data was converted into UV indices, the pressure was converted into altitude and the count data was normalized to counts/min to allow for comparisons with existing results. The processed data is presented in the following figures. The first few points recorded may be from testing the payload prior to launch to ensure system functionality, data during ascent is certainly launch data.

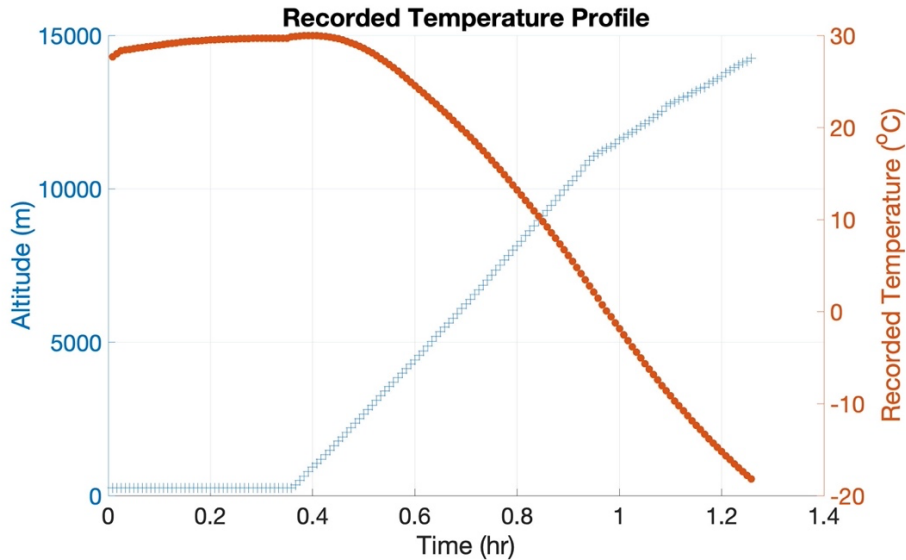


Fig. 6. Payload internal temperature profile with altitude profile, recorded by MS5611.

As seen in Fig. 6, the internal temperature drops significantly during ascent, reaching a final recorded temperature of -18.2 C.

As the payload was stored in the shade, the recorded UV index is low until launch, after which it gradually decreases (shown in Figures 7 and 8). Normally, the UV index would increase with altitude, as there's less atmosphere to filter the UV radiation [17]. The observed decrease is presumably due to the reduction in solar radiation experienced during the eclipse, given that the UV index appears to approach zero at about the rate the eclipse approaches totality.

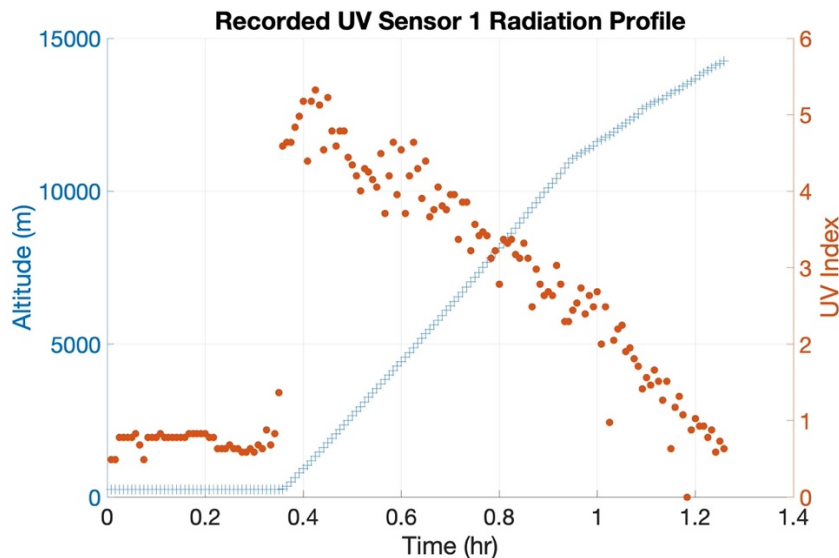


Fig. 7. Balloon UV sensor 1 radiation profile with altitude profile.

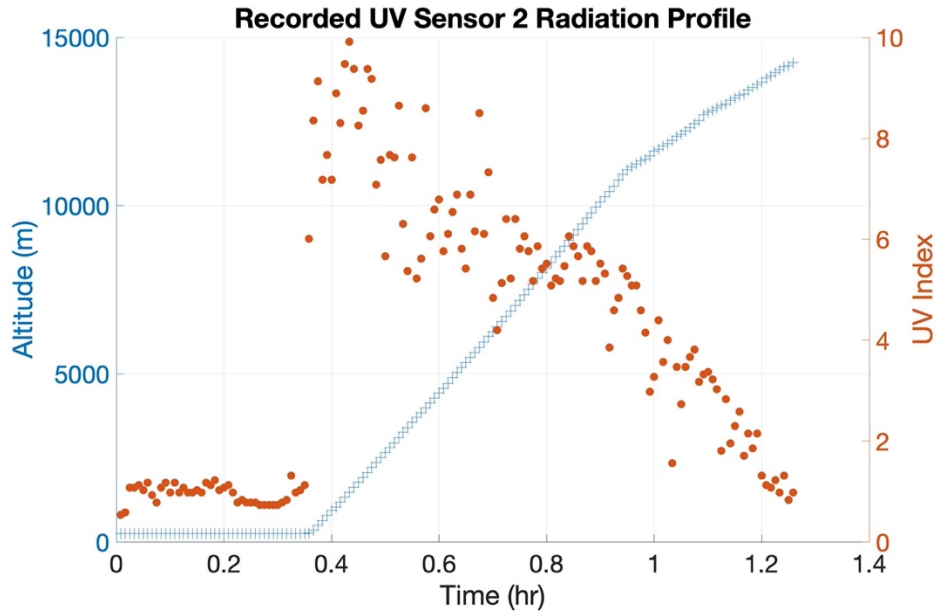


Fig. 8. Balloon UV sensor 2 radiation profile with altitude profile.

The high energy radiation profile recorded (Figures 9 and 10) is very similar to the profile presented in [3]. Compared to [4], there is a scaling difference, but the overall shape is similar. Since GM Counters work by ionizing gas molecules in tubes [3], the scaling difference is likely due to a difference in tube size, as more particles will enter larger tubes. Since the high energy radiation profile is very similar to [3], which was not launched during an eclipse, it does seem that high energy radiation counts are unaffected by the solar eclipse, which is reasonable as this radiation primarily does not originate from the Sun.

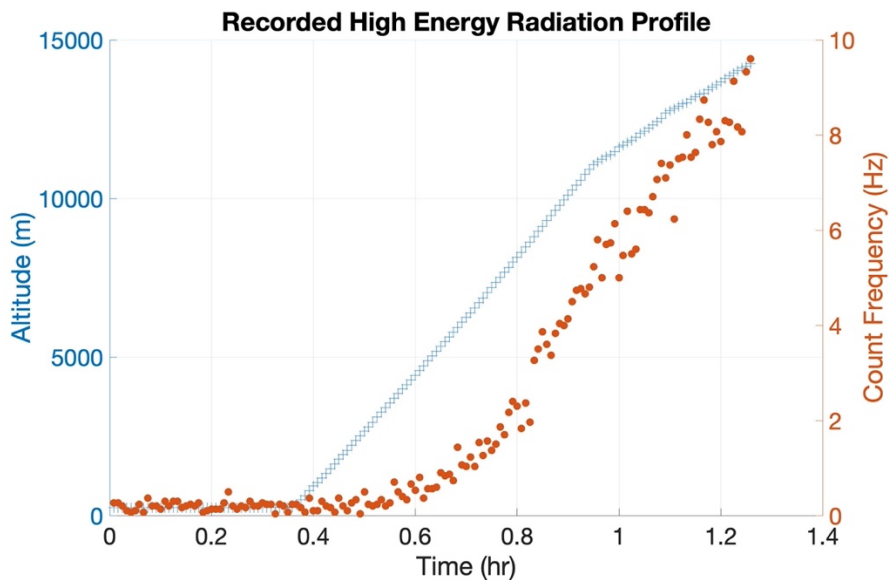


Fig. 9. Balloon high energy radiation profile with altitude profile.

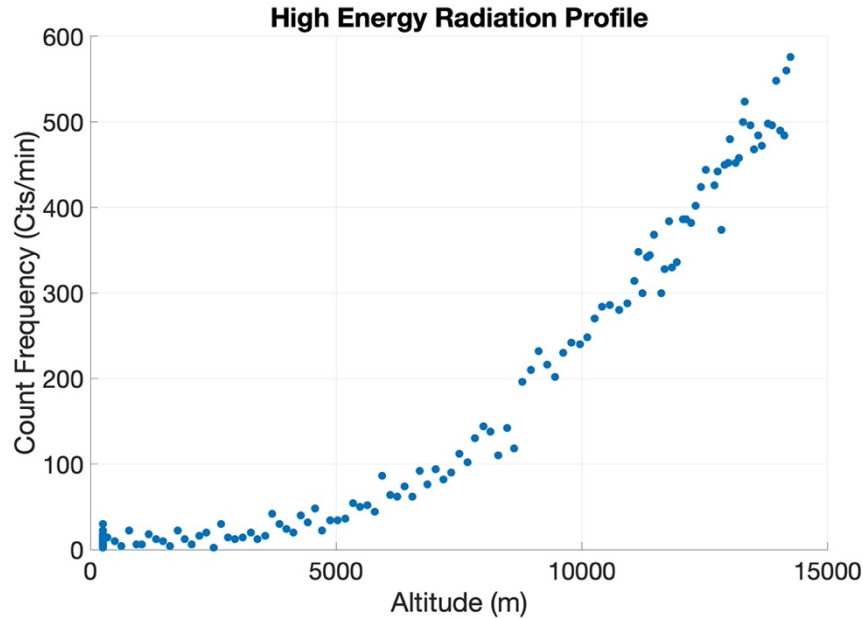


Fig. 10. High energy particle count frequency vs. Altitude in counts/min.

4. Conclusions & Future Steps

While the payload did not log data during and after totality, the ascent component of the high energy radiation pattern obtained by [3-4] is still upheld with this data. Furthermore, the observed UV index decreased with time, in agreement with the authors' understanding of what occurs during a solar eclipse. The payload served as an inexpensive, open-source platform for logging radiation information at high altitudes.

To improve this payload, the battery will be switched from a 9 V battery to 6 AA batteries which should provide a higher capacity. This should prevent the payload from running out of power mid-flight. Another potential improvement is to fly a gamma ray spectrometer instead of a GM Counter, as this would provide energy resolution, allowing for one to determine the energies and counts of high energy particles, instead of just counts as described by [3]. Perhaps a circular payload may also be beneficial for collection of UV index data, with more UV sensors, to reduce chances of data being incorrect due to the payload pointing away from the Sun, which could be a problem with the current box design. Taking inspiration from the custom hardware developed by [1-2], it is also worthwhile to develop a custom radiation sensing module both for open-source replication and education.

5. Acknowledgements

The authors thank Dr. Mary L. Bowden for her support in the development of this payload, as well as for arranging the practice and final eclipse launches. The authors also thank the Maryland Space Grant Consortium for providing funding. Finally, the authors would also like to thank Akemi Takeuchi for providing the full balloon altitude profile (Figure 5), Meredith Embrey for providing information on the GM counter module, Yimang (George) Tang for providing general paper feedback, the UMD-BPP team for their involvement in the eclipse launch and recovery team, who were sent out to recover the payloads from the forest.

References

- 1 REGENER, E. New Results in Cosmic Ray Measurements. *Nature* **132**, 696–698 (1933).
<https://doi.org/10.1038/132696a0>
- 2 Adams, A., Brauer, E. & Stroman, J., (2011) “A Small Geiger Counter Array”, *Academic High Altitude Conference* 2011(1). doi: <https://doi.org/10.31274/ahac.5605>
- 3 B. Holland et al. High Altitude Cosmic Ray Radiation Detection.
https://www.colorado.edu/center/spacegrant/sites/default/files/attached-files/03_High_Altitude_Cosmic_Ray_Radiation_Detection.pdf
- 4 Singam, C. , Burnett, Z. , Renegar, L. & Weinberg, B. (2017) “High Altitude Balloon Operation During 2017 Solar Eclipse”, *Academic High Altitude Conference*. 2017(1). doi: <https://doi.org/10.31274/ahac.3455>
- 5 McIntosh, G., Swanson, A., Taylor, L., Agrimson, E. P., Smith, K. & Xiong, A., (2021) “The Regener-Pfotzer Maximum During a Total Solar Eclipse”, *Journal of High Altitude Ballooning* 1(1).
doi: <https://doi.org/10.31274/jhab.13031>
- 6 Zabori, B., Hirn, A., Deme, S., Apathy, I., and Pazmandi, T, “Characterization of Cosmic Rays and Direction Dependence in the Polar Region up to 88 km altitude,” *J. Space. Weather Space Clim.*, Vol. 6, 2016, pp. A12:1 - 7.
- 7 Tatischeff, V. et al. Orbits and background of gamma-ray space instruments. arXiv.
<https://arxiv.org/pdf/2209.07316#:~:text=Higher%20energy%20gamma%20Drays%2C%20up,weeks%20in%20the%20best%20case>
- 8 Smith Jr., Hastings A. et al. Gamma-Ray Detectors. <https://sgp.fas.org/othergov/doe/lanl/docs1/00326398.pdf>
- 9 Kuznetsov, J. J., Grammer, D. E., Maas, M., Lee, J. D., Villegas, J. O. & Moran, O., (2023) “T.U.F.F : The Utility of Live Tension Measurements for Scientific Ballooning and Flight Dynamics”, *Academic High Altitude Conference* 2022(1). doi: <https://doi.org/10.31274/ahac.15632>
- 10 Jeremy J. Kuznetsov, Akemi Takeuchi, Daniel Grammer, Michael Kalin, Kruti Bhingradiya and Jack Bishop. "Design, Optimization and Additive Manufacture of Generalized Helium Outflow Unit for Latex Balloons to Float," AIAA 2024-0369. *AIAA SCITECH 2024 Forum*. January 2024.
- 11 Deschaine, K., Garg, C., Hoffman, M., Lebetkin, M., Shipman, M. & Warznak, G., (2023) “The Solar Launched Automatic Power System: A Long-Term Solution for Mid-Flight Power Complications”, *Academic High Altitude Conference* 2022(1). doi: <https://doi.org/10.31274/ahac.15642>
- 12 <https://bpp.umd.edu/archives/Open%20Source%20Hardware/>
- 13 <https://github.com/isyedjr/ASIC>
- 14 How to Convert Pressure and Altitude. <https://www.brisbanehotairballooning.com.au/pressure-and-altitude-conversion/>
- 15 135-104LAF-J01 Discrete Thermistors. Honeywell.
<https://mm.digikey.com/Volume0/opasdata/d220001/medias/docus/579/135-104LAF-J01.pdf>
- 16 Analog UV Light Sensor Breakout – GUVA-S12SD. <https://www.adafruit.com/product/1918>
- 17 Chi-yuen, Hong. How to Measure Sunshine Duration? <https://www.hko.gov.hk/en/education/weather/sunshine-and-uv/00120-ultraviolet-radiation-at-high-altitude.html#:~:text=At%20higher%20altitudes%2C%20the%20thinner,level%20will%20increase%20about%2012%25>.